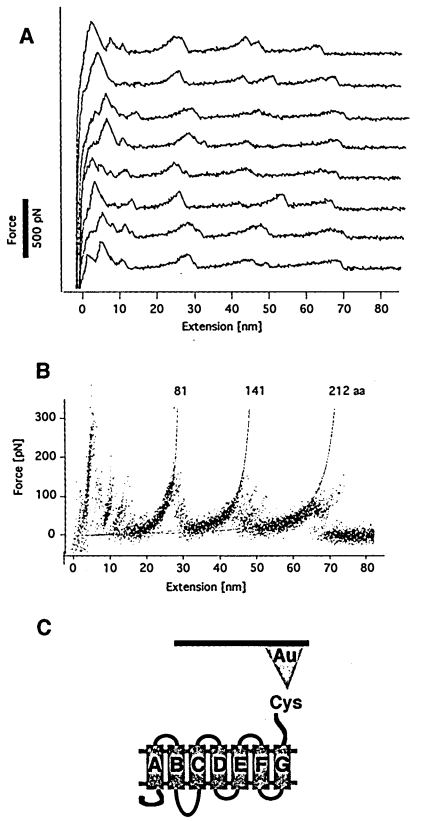

Fig. 5. (**A**) Force spectra of BR mutant G241C with specific anchoring of the COOH-terminus. In G241C, a terminal cysteine was introduced near the COOH-terminus at position 241, allowing specific attachment to a gold evaporated tip. In these experiments, the percentage of full-length force curves increased to 80%. (**B**) Thirty-five force curves are superposed and WLC fits with lengths corresponding to the model shown in Fig. 2 are drawn. In contrast to the measurements in which we used unspecific attachment, we also could resolve the substructure of the first peak, which reflects unfolding of helices F and G.

ing pathways and the local interactions within this membrane protein. In particular, the combination of imaging and spectroscopy enabled us to unravel the individualism of the unfolding processes. Better instruments should allow an even more detailed interpretation of the unfolding pathways of a broad range of membrane proteins such as G proteins and ion channels.

References

1. T. Haltia and E. Freire, *Biochim. Biophys. Acta Bioenerg.* **1228**, 1 (1995).
2. S. H. White and W. C. Wimley, *Annu. Rev. Biophys. Biomol. Struct.* **28**, 319 (1999).
3. S. J. Singer and G. L. Nicolson, *Science* **175**, 720 (1972).
4. G. Binnig, C. F. Quate, C. Gerber, *Phys. Rev. Lett.* **56**, 930 (1986).
5. M. Radmacher, R. W. Tillmann, M. Fritz, H. E. Gaub, *Science* **257**, 1900 (1992).
6. B. Drake *et al.*, *Science* **243**, 1586 (1989).
7. M. Rief, F. Oesterhelt, B. Heymann, H. E. Gaub, *Science* **275**, 1295 (1997).
8. M. Rief, M. Gautel, F. Oesterhelt, J. M. Fernandez, H. E. Gaub, *Science* **276**, 1109 (1997).
9. R. Merkel, P. Nassoy, A. Leung, K. Ritchie, E. Evans, *Nature* **397**, 50 (1999).
10. D. J. Müller, W. Baumeister, A. Engel, *Proc. Natl. Acad. Sci. U.S.A.* **96**, 13170 (1999).
11. A. F. Oberhauser, P. E. Marszalek, H. P. Erickson, J. M. Fernandez, *Nature* **393**, 181 (1998).
12. S. B. Smith, Y. Cui, C. Bustamante, *Science* **271**, 795 (1996).
13. P. Hinterdorfer, W. Baumgartner, H. J. Gruber, K. Schilcher, H. Schindler, *Proc. Natl. Acad. Sci. U.S.A.* **93**, 3477 (1996).
14. U. Dammer *et al.*, *Biophys. J.* **70**, 2437 (1996).
15. U. Dammer *et al.*, *Science* **267**, 1173 (1995).
16. E.-L. Florin, V. T. Moy, H. E. Gaub, *Science* **264**, 415 (1994).
17. G. U. Lee, L. A. Chris, R. J. Colton, *Science* **266**, 771 (1994).
18. A. Engel, H. Gaub, D. J. Müller, *Curr. Biol.* **9**, R133 (1999).
19. A. Engel, C.-A. Schoenenberger, D. J. Müller, *Curr. Opin. Struct. Biol.* **7**, 279 (1997).
20. Y. Zhang, S. Sheng, Z. Shao, *Biophys. J.* **71**, 2168 (1996).
21. Z. Shao and J. Yang, *Q. Rev. Biophys.* **28**, 195 (1995).
22. U. Haupts, J. Tittor, D. Oesterhelt, *Annu. Rev. Biophys. Biomol. Struct.* **28**, 367 (1999).
23. D. Oesterhelt, *Curr. Opin. Struct. Biol.* **8**, 489 (1998).
24. N. Grigorieff, T. A. Ceska, K. H. Downing, J. M. Baldwin, R. Henderson, *J. Mol. Biol.* **259**, 393 (1996).
25. Y. Kimura *et al.*, *Nature* **389**, 206 (1997).
26. E. Pebay-Peyroula, G. Rummel, J. P. Rosenbusch, E. M. Landau, *Science* **277**, 1676 (1997).
27. L.-O. Essen, R. Siegert, W. D. Lehmann, D. Oesterhelt, *Proc. Natl. Acad. Sci. U.S.A.* **95**, 11673 (1998).
28. H. Luecke, H.-T. Richter, J. K. Lanyi, *Science* **280**, 1934 (1998).
29. E. J. M. Helmreich and K.-P. Hofmann, *Biochim. Biophys. Acta* **1286**, 285 (1996).
30. J. M. Baldwin, *EMBO J.* **12**, 1693 (1993).
31. P. A. Hargrave, *Curr. Opin. Struct. Biol.* **1**, 575 (1991).
32. R. Henderson, F. R. S. Shertler, G. F. X. Shertler, *Philos. Trans. R. Soc. London Ser. B* **326**, 379 (1990).
33. J. K. Lanyi, *J. Biol. Chem.* **272**, 31209 (1997).
34. ———, *Nature* **375**, 461 (1995).
35. ———, *Biochim. Biophys. Acta* **1183**, 241 (1993).
36. H. Luecke, B. Schobert, H. Richter, J. Cartailler, J. Lanyi, *Science* **286**, 255 (1999).
37. ———, *J. Mol. Biol.* **291**, 899 (1999).
38. D. J. Müller, M. Amrein, A. Engel, *J. Struct. Biol.* **119**, 172 (1997).
39. D. J. Müller, D. Fotiadis, S. Scheuring, S. A. Müller, A. Engel, *Biophys. J.* **76**, 1101 (1999).
40. D. J. Müller, H.-J. Sass, S. Müller, G. Büldt, A. Engel, *J. Mol. Biol.* **285**, 1903 (1999).
41. D. M. Engelman and T. A. Steitz, *Cell* **23**, 411 (1981).
42. Data not shown.
43. E. Evans and F. Ludwig, *J. Phys. Condens. Matter* **11**, 1 (1999).
44. M. Rief, J. M. Fernandez, H. E. Gaub, *Phys. Rev. Lett.* **81**, 4764 (1998).
45. H. Grubmüller, B. Heymann, P. Tavan, *Science* **271**, 997 (1995).
46. J. B. Heymann *et al.*, *Structure*, in press.
47. M. Pfeiffer, dissertation, Ludwig-Maximilians-Universität München (2000).
48. M. Pfeiffer, T. Rink, K. Gerwert, D. Oesterhelt, H.-J. Steinhoff, *J. Mol. Biol.* **287**, 163 (1999).
49. D. Oesterhelt and W. Stoeckenius, *Methods Enzymol.* **31**, 667 (1974).

9 December 1999; accepted 17 February 2000

Specification of *Drosophila* Hematopoietic Lineage by Conserved Transcription Factors

Tim Lebestky,[1]* Ting Chang,[2]* Volker Hartenstein,[1,2] Utpal Banerjee[1,2,3]†

Two major classes of cells observed within the *Drosophila* hematopoietic repertoire are plasmatocytes/macrophages and crystal cells. The transcription factor Lz (Lozenge), which resembles human AML1 (acute myeloid leukemia–1) protein, is necessary for the development of crystal cells during embryonic and larval hematopoiesis. Another transcription factor, Gcm (glial cells missing), has previously been shown to be required for plasmatocyte development. Misexpression of Gcm causes crystal cells to be transformed into plasmatocytes. The *Drosophila* GATA protein Srp (Serpent) is required for both Lz and Gcm expression and is necessary for the development of both classes of hemocytes, whereas Lz and Gcm are required in a lineage-specific manner. Given the similarities of Srp and Lz to mammalian GATA and AML1 proteins, observations in *Drosophila* are likely to have broad implications for understanding mammalian hematopoiesis and leukemias.

Hematopoietic stem cells give rise to all blood cell lineages in mammals (*1*). Molecular decisions that differentiate one lineage from another are regulated by unique protein complexes constituted of general as well as lineage-specific transcription factors (*2*). Gene inactivation studies in mice have identified an important role for a number of hematopoietic transcription factors. For example, GATA-1 is required for erythroid development (*3*), GATA-2 for definitive hematopoiesis (*4*), and GATA-3 for T cell development (*5*). Interestingly, the *Drosophila* GATA homolog *serpent* (*srp*) is required for embryonic blood cell development (*6*). Another mammalian gene, encoding the AML1 protein, is the most frequent target of chromosomal

[1]Molecular Biology Institute, [2]Department of Molecular, Cell, and Developmental Biology, [3]Departments of Biological Chemistry and Human Genetics, University of California, Los Angeles, CA 90095, USA.

*These authors contributed equally to this report.
†To whom correspondence should be addressed. E-mail: banerjee@mbi.ucla.edu

translocations in acute myeloid leukemias (*7*). AML1, like GATA-2, is essential for all definitive hematopoiesis (*8*). However, the relation between GATA proteins and AML1 in mammals is unclear. The *Drosophila* Lz protein shares 71% identity to AML1 within the Runt domain and regulates the expression of multiple transcription factors during eye development (*9*). Here, we describe the role of Lz in *Drosophila* hematopoiesis and investigate its relation to Srp as well as to another transcription factor, Gcm (*10, 11*), in the generation of *Drosophila* blood cell lineage.

Hemocytes of the *Drosophila* embryo are derived from the head mesoderm (*12*) (Fig. 1, A to C). The hemocyte precursors express the GATA factor Srp (*6, 13*) and give rise to two classes of cells: plasmatocytes and crystal cells (*14*). Plasmatocytes spread throughout the endolymph (Fig. 1, B and C) and act as macrophages, whereas crystal cells contain crystalline inclusions and are involved in the melanization of pathogenic material in the hemolymph (*15*). These cells can be first recognized in the late embryo, where they form a cluster around the proventriculus (Fig. 1, C and G). Crystal cells are made clearly visible by the *Black cell* (*Bc*) mutation, which causes premature melanization of the crystalline inclusions (*16*).

In larval stages, hemocytes are produced from a separate organ called the lymph gland (*15, 17*). Precursors of this gland first appear during embryogenesis in the dorsal mesoderm of the thoracic segments (*18*) (Fig. 1B). Later, these precursors migrate dorsally, forming a tight cluster adjacent to the dorsal vessel, the larval circulatory organ (Fig. 1C). The larval lymph glands form a bilateral chain of cell clusters ("lobes") flanking the dorsal vessel (Fig. 1D).

In the temperature-sensitive allele lz^{ts1}, crystal cells develop normally at 25°C (Fig. 1, E and G). However, crystal cell development is completely blocked at 29°C (Fig. 1, F and H). Consistent with earlier genetic analysis (*19*), crystal cells are missing in *lz* null mutant alleles (*20*). Plasmatocytes develop normally in number and pattern in *lz* null embryos (*21*).

Temperature shifts of lz^{ts1}; *Bc* flies showed that Lz function during stages 10 to 14 of embryogenesis is essential for crystal cell development (*22*). Crystal cells formed in the embryo do not persist into late larvae, and Lz function is continuously required during the late larval stages for further crystal cell development. The time scale for de novo crystal cell development in the larva is about 4.5 hours (*22*).

Lz is first detected in a small cluster of cells within the embryonic head mesoderm in a bilaterally symmetric pattern (Fig. 2A) (*23*). Lz expression remains localized in bilateral clusters of 20 to 30 cells within the head mesoderm (Fig. 2, B and C). At later stages, these crystal cell precursors (CCPs) form a loose cluster around the proventriculus (Fig. 2D). These cells have smooth, round morphology with large nuclei (Fig. 2E). The CCPs form a subset of the Srp-expressing hemocyte precursors (Fig. 2, F to H).

Colocalization with a mitotic marker suggests that Lz-expressing cells can divide (Fig. 2I). Interestingly, not all of the daughter cells from these divisions will become crystal cells. This is inferred from the observation that *lz-lacZ* expression is also seen in a group of plasmatocytes (Fig. 2J) that do not express *lz* mRNA or Lz protein. We interpret the expression of *lz-lacZ* in these cells to be due to the long half-life of β-galactosidase protein that is left over from the parent cell. This is also observed with additional, independent *lz* promoter fusions to *lacZ* (*20*). Thus, Lz is expressed in a small subset of hemocyte precursors that may undergo cell division. All crystal cells resulting from these precursors maintain Lz expression. The few daughter cells that will differentiate into plasmatocytes do not express Lz protein.

In the larval lymph gland, Lz expression is initiated in a small number of cells during the second larval instar (Fig. 3A) (*24*). The number of cells expressing Lz steadily increases during the third larval instar, reaching 50 to 100 cells per lobe (Fig. 3, B and C). Lz-expressing cells are scattered uniformly throughout the large, primary lobe of the lymph gland, whereas the smaller secondary lobes do not express Lz. Similar to the embryonic head mesoderm, all lymph gland cells express Srp, but only a small subset of them express Lz (Fig. 3, D to F). Interestingly, the Lz-expressing cells appear to down-regulate Srp when compared to the surrounding non–Lz-expressing hemocyte precursors (inset, Fig. 3, D and E).

Immunolocalization studies (*25*) of circulating hemocytes in third-instar larvae suggest that the expression of Lz protein is maintained in circulating crystal cells (*21*). Given that crystal cells are missing in *lz* mutants, this demonstrates an autonomous requirement for Lz in crystal cell development. As observed for embryonic hemocytes, Lz-ex-

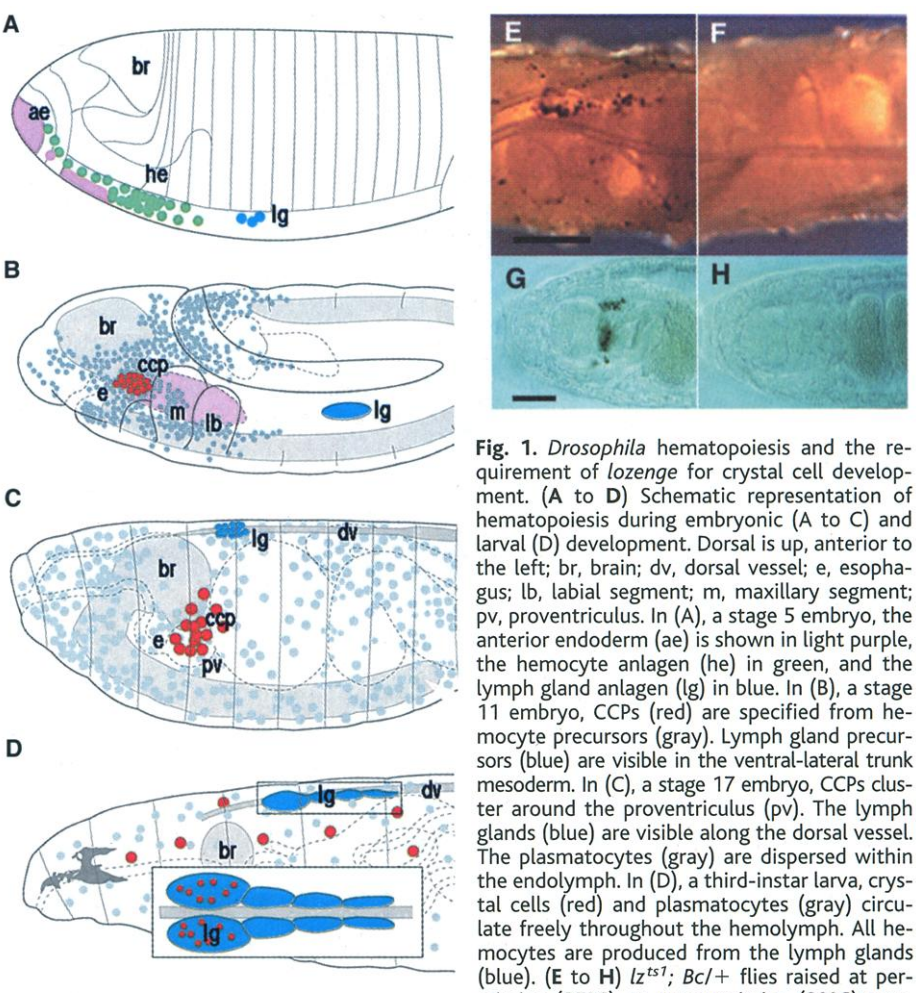

Fig. 1. *Drosophila* hematopoiesis and the requirement of *lozenge* for crystal cell development. (**A** to **D**) Schematic representation of hematopoiesis during embryonic (A to C) and larval (D) development. Dorsal is up, anterior to the left; br, brain; dv, dorsal vessel; e, esophagus; lb, labial segment; m, maxillary segment; pv, proventriculus. In (A), a stage 5 embryo, the anterior endoderm (ae) is shown in light purple, the hemocyte anlagen (he) in green, and the lymph gland anlagen (lg) in blue. In (B), a stage 11 embryo, CCPs (red) are specified from hemocyte precursors (gray). Lymph gland precursors (blue) are visible in the ventral-lateral trunk mesoderm. In (C), a stage 17 embryo, CCPs cluster around the proventriculus (pv). The lymph glands (blue) are visible along the dorsal vessel. The plasmatocytes (gray) are dispersed within the endolymph. In (D), a third-instar larva, crystal cells (red) and plasmatocytes (gray) circulate freely throughout the hemolymph. All hemocytes are produced from the lymph glands (blue). (**E** to **H**) lz^{ts1}; *Bc*/+ flies raised at permissive (25°C) or nonpermissive (29°C) temperature. In (E), a third-instar larva raised at 25°C displays a normal distribution of crystal cells (arrowhead). In (F), a third-instar larva raised at 29°C lacks crystal cells. In (G), a stage 17 embryo raised at 25°C, crystal cells (arrowhead) are clustered around the proventriculus. In (H), a stage 17 embryo raised at 29°C, crystal cells are absent. Scale bars, 300 μm (E and F), 50 μm (G and H).

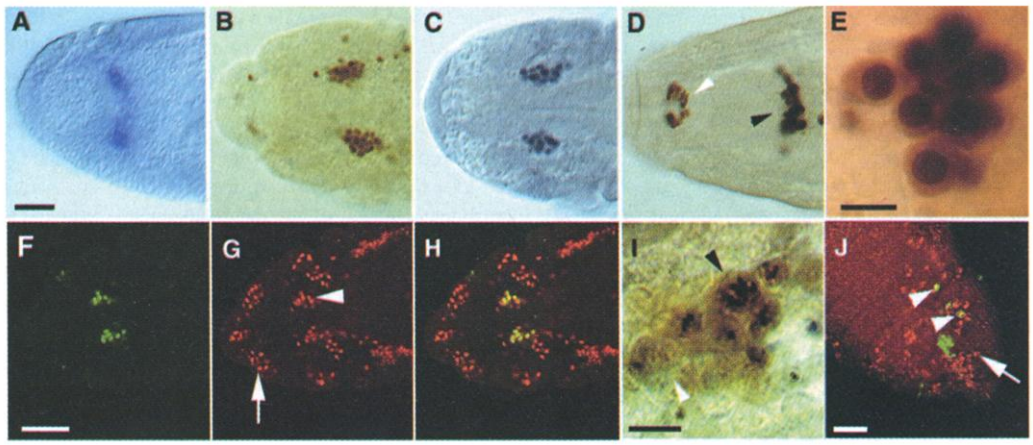

Fig. 2. Expression of Lz during embryonic hematopoiesis. (**A** to **C**) Dorsal views. In (A), a stage 10 embryo shows in situ localization of *lz* mRNA. In (B), a stage 12 *lz-gal4/+; UAS-NlacZ /+* embryo shows immunolocalization of a nuclear form of β-Gal in a *lz* pattern. In (C), a stage 13 embryo shows immunolocalization of Lz protein. (**D** to **H**) *lz-gal4/+; UAS-NlacZ/+* embryos. Immunolocalization of β-Gal protein is shown (brown in D and E, green in F and H). In (D), a stage 17 embryo, the black arrowhead denotes the Lz-expressing cluster of crystal cells around the proventriculus. A white arrowhead points to expression of Lz in the gnathal region, which is unrelated to the expression in the CCPs and has no known phenotypic consequences. In (E), a stage 17 embryo at higher magnification shows Lz expression. Note the large nuclei and the round morphology of the crystal cells. In (F), a stage 13 embryo shows Lz expression (green). In (G), the same section as in (F) shows immunolocalization of Srp (red); an arrowhead marks the position of a CCP cluster, and an arrow points to circulating plasmatocytes. In (H), a merged image of (F) and (G) displays colocalization of Lz and Srp (yellow). (**I**) Stage 11 *lz-gal4; UAS-lacZ* embryo showing immunolocalization of phospho-Histone H3A (black) and cytoplasmic β-Gal (brown). A white arrowhead marks a nondividing β-Gal–expressing cell; a black arrowhead marks colocalization of phospho-Histone H3A (black) and β-Gal (brown) in a dividing cell. (**J**) Stage 13 *lz-gal4; UAS-lacZ* embryo showing expression of the plasmatocyte-specific marker Croquemort (red) in circulating embryonic plasmatocytes. An arrow points to Croquemort expression in a plasmatocyte that lacks expression of β-Gal. Arrowheads point to plasmatocytes that express both Croquemort and β-Gal (green). Scale bars, 50 μm (A to D and F and J), 8 μm (E and I).

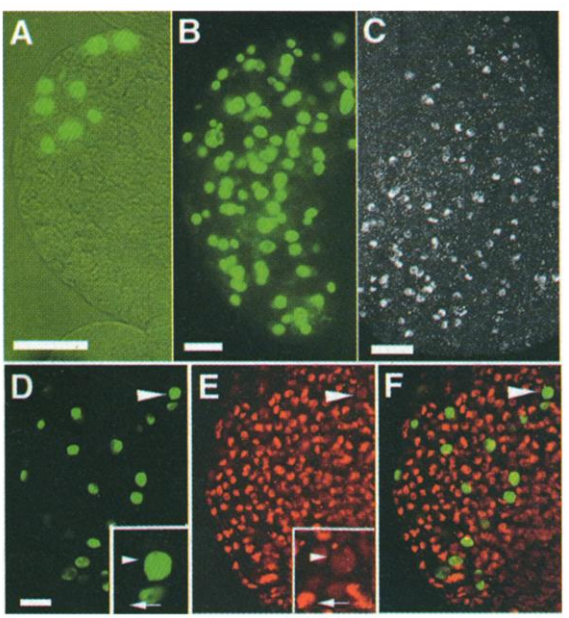

Fig. 3. Expression of Lz during larval hematopoiesis in *lz-gal4/+; UAS-NlacZ/+* (**A**, **B**, **D** to **F**) and wild-type (**C**) larvae. Immunolocalization of β-Gal is shown as a reporter for Lz (green) and Srp (red). Lz expression is revealed within a single anterior lobe of a second-instar larval lymph gland (A) and within a single anterior lobe of a third-instar larval lymph gland (B). Immunolocalization (with antibody to Lz) of Lz protein expression in a single anterior lobe of a third-instar larval lymph gland is shown in (C). Expression is similar to *lz* reporter expression seen in (B). A 1-μm confocal optical section of a single lobe of a third-instar larval lymph gland is shown in (D); an arrowhead points to a Lz-expressing cell (magnified in inset), and an arrow points to a cell lacking Lz expression. In (E), the same section as in (D) shows Srp protein expression; an arrowhead points to a cell expressing both Srp and Lz (magnified in inset), and an arrow points to a cell expressing high levels of Srp but no Lz. In (F), a merged image of (D) and (E) displays colocalization of Lz and Srp. Scale bars, 25 μm (A), 50 μm (B to D).

pressing precursors give rise to all crystal cells and a small subset of plasmatocytes, as evidenced by morphology as well as expression of the plasmatocyte marker Croquemort (*21*). However, Lz protein is not observed in any circulating larval plasmatocytes.

An allele of *srp* (srp^{neo45}) specifically abolishes Srp expression in embryonic hemocytes (*6*). Because this allele also eliminates *lz* mRNA expression, Srp function is required for the expression of Lz (Fig. 4, A and B). This finding establishes that *srp* functions upstream of *lz* during embryonic hematopoiesis. The lethality of *srp* precludes the analysis of Lz expression in larval lymph glands of *srp* mutants. However, as in the embryo, Srp is expressed earlier than Lz in the larval hemocyte precursors, which suggests that *srp* acts upstream of *lz* during both developmental stages.

The transcription factor Gcm promotes glial cell fate, and it also functions downstream of Srp in plasmatocyte differentiation (*10*). Lz expression is unaffected in *gcm* mutants (Fig. 4C). Gcm expression (*26*) is initiated in a number of Srp-expressing hemocyte precursors (Fig. 4, D to F), but Gcm is excluded from the CCPs (Fig. 4, G to I). Consistent with their cell fate, the small subset of plasmatocytes derived from Lz-expressing progenitors do initiate Gcm expression (*21*).

We misexpressed Gcm in the CCPs to assess whether exclusion of Gcm from these cells is essential for proper fate determination. This resulted in the transformation of CCPs into plasmatocytes (Fig. 4, J, K, L, and N). The converted cells exhibit morphological characteristics of plasmatocytes (Fig. 4N) and express Croquemort (Fig. 4, J to L). Moreover, in third-instar larvae, misexpression of Gcm in CCPs prevents the development of all crystal cells (Fig. 4O). These results suggest that the restricted expression of Gcm is required for the developmental program of embryonic plasmatocytes, and that its misexpression can override Lz-mediated crystal cell differentiation during both embryonic and larval hematopoiesis. The converse experiment of Lz misexpression in the entire hemocyte pool under the control of a heat shock promoter did not convert plasmatocytes into crystal cells (*20*). Vertebrate homologs of Gcm have been identified (*27*), but any role in hematopoiesis has not been investigated.

We arrive at a model of *Drosophila* hematopoiesis (Fig. 4P) in which a pool of Srp-positive hemocyte precursors gives rise to a large population of Gcm-positive cells and a smaller subpopulation of Lz-positive cells. Our results support a genetic hierarchy in which Srp, a *Drosophila* GATA factor, acts upstream of both Gcm and Lz, two mutually exclusive, lineage-specific transcription factors in hematopoiesis. Although the description of this hierarchy is incomplete in terms of the breadth of molecules involved, it does provide a theoretical framework for understanding how early hematopoietic progenitors in the embryo can differentiate and assume distinct cell fates.

Recent findings have identified similarities between mammalian and *Drosophila* innate immunity (*28*). Given the similarities of

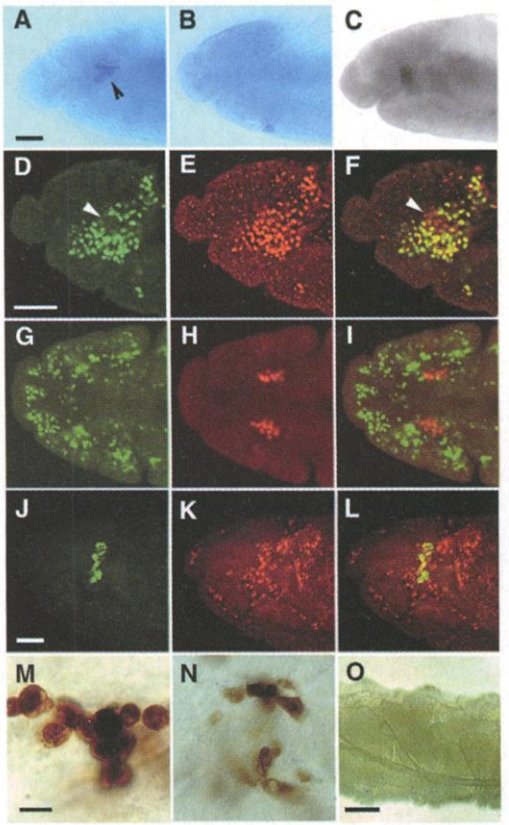

Fig. 4. Functional relations among Srp, Lz, and Gcm. (**A** and **B**) In situ localization of *lz* mRNA expression (arrowhead) in the head mesoderm of stage 13 $srp^{neo45}/+$ (A) and srp^{neo45}/srp^{neo45} (B) embryos. Lz expression is absent in srp^{neo45}/srp^{neo45} embryos. (**C**) Immunolocalization of Lz protein in stage 11 $gcm^{N7\text{-}4}$ embryo. Lz expression is unaffected in *gcm* mutants. (**D** to **F**) Stage 11 *gcm-lacZ*/+ embryo. In (D), Gcm (green) is expressed in a majority of the hemocyte precursors; an arrowhead points to a gap in Gcm expression. In (E), Srp protein (red) is expressed in all hemocyte precursors. In (F), a merged image of (D) and (E) shows that Srp and Gcm do not colocalize in a small field of cells (arrowhead) presumed to be the CCPs. (**G** to **I**) Stage 13 *gcm-lacZ*/+ embryo. In (G), Gcm (green) is expressed in the majority of hemocyte precursors. In (H), Lz protein (red) is expressed in the CCPs. In (I), a merged image of (G) and (H), Lz and Gcm are mutually exclusive. (**J** to **L**) Stage 14 *lz-gal4/+; UAS-lacZ/+; UAS-gcm* embryo. In this genotype, Gcm protein is misexpressed in CCPs. In (J), Lz (green) is expressed in the head mesoderm. In (K), Croquemort (red) is expressed in plasmatocytes. In (L), a merged image of (J) and (K) shows that misexpression of Gcm results in expression of Croquemort in the Lz-expressing cells of the head mesoderm, indicating transformation of CCPs into plasmatocytes. (**M**) Stage 17 *lz-gal4/+; UAS-NlacZ/+* embryo, showing the smooth round morphology of the crystal cells. (**N**) Stage 17 *lz-gal4/+; UAS-lacZ/+; UAS-gcm* embryo. The Lz-expressing cells that also express Gcm show altered morphology resembling circulating plasmatocytes. (**O**) Third-instar *lz-gal4/+; Bc/UAS-gcm* larva. Misexpression of Gcm in larval CCPs causes a complete loss of mature crystal cells in the hemolymph. (**P**) Model for the generation of hematopoietic lineages in the *Drosophila* embryo. Srp is expressed earliest in the hemocyte precursor pool. Most of the Srp-expressing cells begin to express Gcm and differentiate as plasmatocytes. A small subset of Srp-expressing cells begin to express Lz; these cells are still mitotic and give rise to all the crystal cells and a very small fraction of the plasmatocytes. Scale bars, 50 μm (A and B, D to I, J to L), 8 μm (M and N), 200 μm (O).

Srp and Lz to mammalian GATA and AML1 proteins, the results reported here suggest a conservation of the molecular basis for blood cell lineage commitment in mammalian and *Drosophila* hematopoiesis.

References and Notes

1. S. H. Orkin, *Int. J. Dev. Biol.* **42**, 927 (1998).
2. M. H. Sieweke and T. Graf, *Curr. Opin. Genet. Dev.* **8**, 545 (1998).
3. Y. Fujiwara, C. P. Browne, K. Cunniff, S. C. Goff, S. H. Orkin, *Proc. Natl. Acad. Sci. U.S.A.* **93**, 12355 (1996).
4. F. Y. Tsai and S. H. Orkin, *Blood* **89**, 3636 (1997).
5. C. N. Ting, M. C. Olson, K. P. Barton, J. M. Leiden, *Nature* **384**, 474 (1996).
6. K. P. Rehorn, H. Thelen, A. M. Michelson, R. Reuter, *Development* **122**, 4023 (1996).
7. T. H. Rabbitts, *Nature* **372**, 143 (1994).
8. Q. Wang *et al.*, *Proc. Natl. Acad. Sci. U.S.A.* **93**, 3444 (1996); T. Okuda, J. van Deursen, S. W. Hiebert, G. Grosveld, J. R. Downing, *Cell* **84**, 321 (1996); N. A. Speck *et al.*, *Cancer Res.* **59**, 1789s (1999); S. Bae and Y. Ito, *Histol. Histopathol.* **14**, 1213 (1999).
9. A. Daga, C. A. Karlovich, K. Dumstrei, U. Banerjee, *Genes Dev.* **10**, 1194 (1996); G. V. Flores, A. Daga, H. R. Kalhor, U. Banerjee, *Development* **125**, 3681 (1998).
10. R. Bernardoni, B. Vivancos, A. Giangrande, *Dev. Biol.* **191**, 118 (1997).
11. T. Hosoya, K. Takizawa, K. Nitta, Y. Hotta, *Cell* **82**, 1025 (1995); B. W. Jones, R. D. Fetter, G. Tear, C. S. Goodman, *Cell* **82**, 1013 (1995).
12. U. Tepass, L. I. Fessler, A. Aziz, V. Hartenstein, *Development* **120**, 1829 (1994).
13. V. Riechmann, K. P. Rehorn, R. Reuter, M. Leptin, *Development* **125**, 713 (1998).
14. B. Mathey-Prevot and N. Perrimon, *Cell* **92**, 697 (1998); C. R. Dearolf, *Biochim. Biophys. Acta* **1377**, M13 (1998).
15. T. M. Rizki, in *Genetics and Biology of* Drosophila, M. Ashburner and T. R. F. Wright, Eds. (Academic Press, London, 1978), vol. 2b, pp. 398–451.
16. T. Rizki, R. Rizki, E. Grell, *Roux's Arch. Dev. Biol.* **188**, 91 (1980).
17. R. Shresta and E. Gatteff, *Dev. Growth Differ.* **24**, 65 (1982).
18. A. E. Rugendorff, A. Younossi-Hartenstein, V. Hartenstein, *Roux's Arch. Dev. Biol.* **203**, 266 (1993).
19. T. Rizki and R. Rizki, *Genetics* **97**, s90 (1981).
20. T. Lebestky, T. Chang, V. Hartenstein, U. Banerjee, data not shown.
21. For further details, see *Science* Online (www.sciencemag.org/feature/data/1047010.shl).
22. Embryos were collected for 2 hours at either 25°C (for up-shift experiments) or 29°C (for down-shift experiments), and shifted either up or down at stages 8, 10, 11, 13, 14, and 15. Completion of embryogenesis takes about 22 hours at 25°C and 16 hours at 29°C. The ratio of 16/22 was used to compensate for this timing differential in the down-shift experiments. When shifted down at stages 8 and 10, black cells were still present within the embryos analyzed at stage 17. When shifted down at stages 11, 13, 14, and 15, black cells were absent from the embryos at stage 17. When shifted up to 29°C at stages 8, 10, 11, 13, and 14, black cells were absent from the embryos at stage 17, but when shifted up at stage 15, black cells were present in stage 17 embryos. These results suggest that Lz function is required continuously between stages 10 and 14 for crystal cell development. Furthermore, when lz^{ts1}; *Bc*/+ embryos develop at 25°C until stage 17, but are then shifted to 29°C during larval stages, no crystal cells are observed in the third-instar larvae, indicating that embryonic crystal cells do not persist into late larval stages. Additionally, when lz^{ts1}; *Bc*/+ embryos are raised at 29°C until third-instar larvae and are shifted to 25°C, crystal cells appear within 4.5 hours after the restoration of Lz function.
23. Antisense *lz* mRNA probe was made from the 3.5-kb *lz* cDNA (9). Rabbit antibody to Lz (9) was used at 1:50 dilution. Affinity-purified mouse antibody to Lz was used at 1:100 dilution. In situ hybridization and immunohistochemistry protocols were as described (12).
24. Lymph glands were dissected by cutting at 7/8 length along the larval body. Using fine tweezers, the inner tissue was inverted and lymph glands were separated from surrounding tissue. Lymph glands were fixed and stained using protocols derived from eye disc staining protocols as described (9).
25. Smears of circulating hemocytes from third-instar hemolymph were created by cutting larvae with fine tweezers and depositing the hemolymph on a glass slide. For immunolocalization, smears were fixed in 0.5% glutaraldehyde for 30 s, rinsed with PBT (PBS + 0.05% Triton) five times, incubated in PBT-N (PBS + 0.05% Triton + 10% normal goat serum) for 1 min, incubated in primary antibody overnight at 4°C, rinsed in PBT five times, washed in PBT-N for 1 min, incubated in secondary antibody for 2 hours at room temperature, rinsed five times in PBT, and mounted in Vectashield (Vector Laboratories) fluorescent mounting medium.
26. The *gcm-lacZ* referenced in the text and legends is the gcm^{rA87} enhancer trap allele. Similarly, *lz-lacZ* refers to the *lz-gal4; UAS-lacZ* genotype.
27. J. Kim *et al.*, *Proc. Natl. Acad. Sci. U.S.A.* **95**, 12364 (1998); Y. Kanemura *et al.*, *FEBS Lett.* **442**, 151 (1999); Y. Akiyama, T. Hosoya, A. M. Poole, Y. Hotta, *Proc. Natl. Acad. Sci. U.S.A.* **93**, 14912 (1996).
28. J. A. Hoffmann, F. C. Kafatos, C. A. Janeway, R. A. B. Ezekowitz, *Science* **284**, 1318 (1999).

29. We thank R. Reuter for useful discussions, the Srp antibody, and the srp^{neo45} allele; L. Fessler and J. Fessler for helpful suggestions and discussions; N. Franc for providing Croquemort antibody; A. Giangrande for useful discussions, *UAS-gcm* and gcm^{rA87}, and Gcm antibody; C. Goodman and B. Jones for Gcm antibody; J. Pollock for the *lz-gal4* stock; K. Matthews at the Bloomington Stock Center for many fly stocks; members of the Banerjee lab for critical review and comments on the manuscript; and E. Chan for his involvement in early stages of the project. Supported by U.S. Public Health Service National Research Service Award GM07185 (T.L.); NIH grant RO1EY08152, the McKnight Foundation Investigator Award, and the Margaret E. Early Medical Research Trust Award (U.B.); and NIH grant NS29367 (V.H.).

11 November 1999; accepted 2 February 2000